

Synthesis and Characterization of Ni²⁺-doped TiO₂ Nanowires

Trinh Thi Loan*, Vu Hoang Huong, Tran Thi Dung, Nguyen Ngoc Long

Faculty of Physics, VNU University of Science, 334 Nguyen Trai, Thanh Xuan, Hanoi, Vietnam

Received 19 September 2016

Revised 28 September 2016; Accepted 30 September 2016

Abstract: TiO₂ nanowires doped with different amounts of Ni²⁺ ions (from 0 to 18 mol%) were synthesized by hydrothermal technique. The samples were characterized by X-ray diffraction (XRD) and Raman spectroscopy, field emission scanning electron microscopy (FESEM), and diffuse reflection spectroscopy. The XRD analysis showed that the doped samples exhibit anatase single phase. The lattice parameters remain unchanged, independent on Ni²⁺ content. Diameter of TiO₂ nanowires increased significantly with increasing concentrations of Ni²⁺. The investigated results indicate that a greater portion of the Ni²⁺ ions are well-incorporated into the anatase TiO₂ lattice. Indirect and direct band gap energies of Ni²⁺-doped TiO₂ with different doping concentration were found to be in the range from 3.24 to 2.99 eV and 3.54 to 3.35 eV, respectively.

Keywords: TiO₂:Ni²⁺ nanowires, hydrothermal, diffuse reflection, band gap energy.

1. Introduction

In recent few decades, titanium dioxide (TiO₂) is extensively studied by different research centers throughout the world due to its wide applications in such areas as photocatalysis [1], solar energy conversion [2], gas sensing [3], and many others [4, 5]. However, TiO₂ has limited applications under visible light irradiation because of its poor light absorption ability and low charge separation efficiency under normal reaction conditions. This is due to its wide band gap [6, 7]. One effort to improve the light absorption of TiO₂ for efficient utilization of the solar energy spectrum is the doping with transition metals, which inserts a new band into the original band gap of TiO₂ or modifies the conduction band (CB) or the valence band (VB) of TiO₂ [8].

In this article, we synthesized TiO₂ nanowires doped with different amounts of Ni²⁺ ions (from 0 to 18 mol%) by hydrothermal technique. The prepared samples are investigated using developed techniques such as X-ray diffraction (XRD), Raman, FESEM and diffuse reflection to find out the influence of Ni²⁺ doping on the structure, morphology and optical features of the samples.

2. Experimental

The TiO₂ nanowires doped with different amounts of Ni²⁺ ions (from 0 to 18 mol%) were synthesized by hydrothermal technique using 10 M NaOH aqueous solution, anatase TiO₂ powders,

*Corresponding author. Tel.: 84-904367699
Email: loan.trinhthi@gmail.com

0.02 M $\text{Ni}(\text{NO}_3)_2$ aqueous solution and urea powder as the precursors. The typical procedure was as follows: 0.6 g urea was dissolved in 80 ml of 10 M solution of NaOH. Then, 0.8 g of TiO_2 was dispersed in the above solution followed by steady stirring for 15 min. Then, an appropriate quantity of 0.02 M solution of $\text{Ni}(\text{NO}_3)_2$ was added to the above mixed solution followed by continuous steady stirring. The solution was transferred into Teflon-lined steel autoclave. The autoclave then was put in a drying cabinet and kept at temperature of 200 °C for 36 h and then cooled naturally to room temperature. Thereafter, the precipitate was filtered and washed with HCl and distilled water, and then was poured back into Teflon-lined steel autoclave with 80 ml of distilled water and kept at temperature of 160 °C for 15 h. Finally, the precipitate was filtered and dried in air at 120 °C for 24 h.

The crystalline phase of Ni^{2+} -doped TiO_2 was studied by a Siemens D5005 Bruker, Germany X-ray diffractometer (XRD) with $\text{Cu-K}\alpha 1$ irradiation ($\lambda = 1.54056 \text{ \AA}$). Raman spectra were measured using LabRam HR800, Horiba spectrometer with 632.8 nm excitation. Nova Nano SEM 450, FEI field emission scanning electron microscope (FESEM) with the energy dispersive X-ray spectrometer (EDS) was used to observe the sample morphologies and elemental composition analysis. Diffuse reflection spectroscopy measurements were carried out on a VARIAN UV-VIS-NIR Cary-5000 spectrophotometer. The Kubelka-Munk function $F(R)$ proportional to the absorption coefficient was calculated using the equation: $F(R) = (1-R)^2/(2R) = K/S$, where R , K and S are the reflection, the absorption and the scattering coefficient, respectively.

3. Results and discussion

3.1. Structure characterization

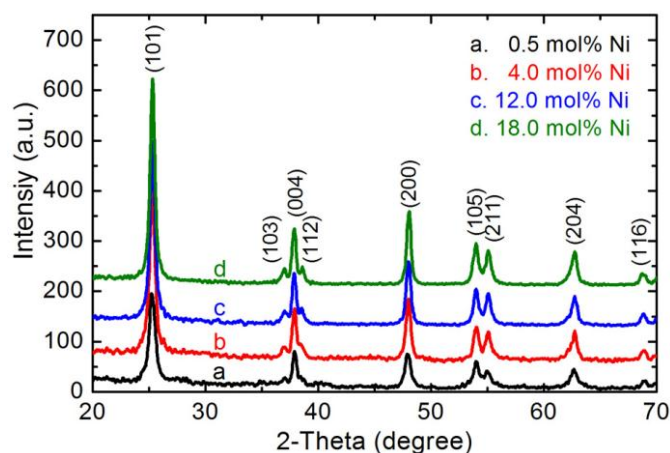


Fig.1. XRD patterns of the Ni^{2+} -doped TiO_2 samples with different doping concentration.

Fig.1 presents the XRD patterns of Ni^{2+} -doped TiO_2 samples with different doping concentration. It can be seen that all samples show only anatase single phase regardless of Ni^{2+} content. In each pattern, the nine peaks lying at 2θ angles: 25.32, 37.02, 37.89, 38.58, 48.06, 53.97, 55.05, 62.73, and 68.70° were observed. These peaks correspond to the (101), (103), (004), (112), (200), (105), (211), (204), and (116) planes of anatase phase with tetragonal geometry, respectively (JCPDS card: 04-0477). The lattice parameters of samples calculated from the XRD patterns are shown in Table 1. The lattice parameters remain unchanged, independent on Ni^{2+} content. This is evident considering that

Ni^{2+} has an ionic radius similar to Ti^{4+} and can also form octahedral coordination as Ti^{4+} does [9]. When comparing to bulk anatase TiO_2 ($a = b = 3.784 \text{ \AA}$ and $c = 9.514 \text{ \AA}$), a variation in c lattice constant has been observed for the prepared samples as shown in Table 1. The reason for this may be due to the tensile strain in the lattice.

Table 1. The lattice parameters of the $\text{TiO}_2:\text{Ni}^{2+}$ samples with different doping concentration.

Ni^{2+} content (mol%)	d_{101} (Å)	d_{004} (Å)	d_{200} (Å)	d_{204} (Å)	$a = b$ (Å)	c (Å)
0.5	3.517	2.373	1.891	1.479	3.782 ± 0.001	9.493 ± 0.002
4.0	3.516	2.374	1.893	1.480	3.787 ± 0.001	9.497 ± 0.004
12.0	3.521	2.371	1.894	1.479	3.788 ± 0.005	9.487 ± 0.002
18.0	3.522	2.372	1.894	1.481	3.789 ± 0.002	9.493 ± 0.007

It is well known that the conventional crystallographic unit cell of anatase TiO_2 is tetragonal geometry (space group $I4_1/amd$) and contains two primitive unit cells, each of which contains two formula units of TiO_2 . According to the factor group analysis, six modes of pure anatase TiO_2 , $A_{1g} + 2B_{1g} + 3E_g$, are Raman active and three modes, $A_{2u} + 2E_u$, are infrared active. One vibration, B_{2u} , will be inactive in both infrared and Raman spectra. Thus, group theory predicts six Raman active modes for the tetragonal anatase phase [10]. The Raman active modes of the anatase structure were observed at approximately 144 cm^{-1} ($E_g(1)$), 197 cm^{-1} ($E_g(2)$), 399 cm^{-1} (B_{1g}), 519 cm^{-1} (A_{1g} & B_{1g}) and 639 cm^{-1} ($E_g(3)$) [10, 11]. It has been known that the $E_g(1)$, $E_g(2)$ and B_{1g} modes are the Ti-O bond stretching type vibrations. The A_{1g} , B_{1g} and $E_g(3)$ modes are the O-Ti-O bending type vibrations [10]. The Raman spectra of Ni^{2+} -doped TiO_2 are shown in Fig. 2. The spectra exhibit modes at 142 cm^{-1} ($E_g(1)$), 196 cm^{-1} ($E_g(2)$), 395 cm^{-1} (B_{1g}), 514 cm^{-1} (A_{1g} , B_{1g}) and 638 cm^{-1} ($E_g(3)$). No indication of the presence of rutile or any secondary phases are seen.

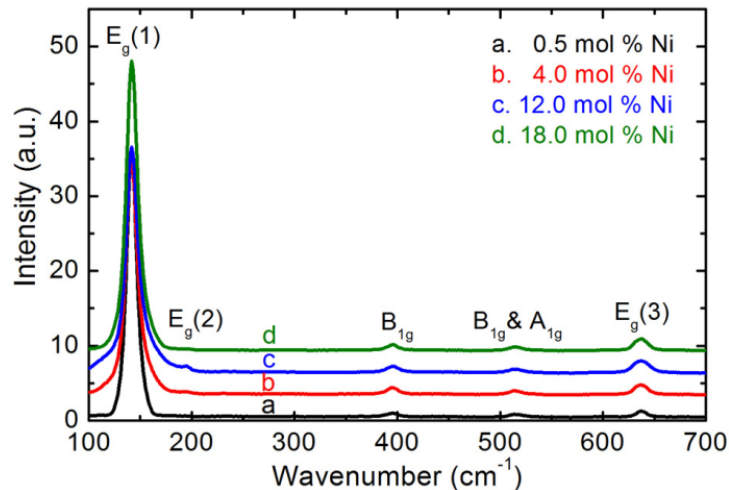


Fig.2. Raman spectra of the Ni^{2+} -doped TiO_2 samples with different doping concentration.

The EDS spectra of the TiO_2 samples doped with 4.0 and 18.0 mol% Ni^{2+} are presented in Fig. 3. The EDS spectra exhibit the peaks related to the Ti, O and Ni elements, in addition, the characteristic peaks for Ni element increase in intensity when Ni^{2+} concentration increases. The results of the EDS analysis indicate that the Ni^{2+} ions are incorporated in Ti^{4+} lattice sites.

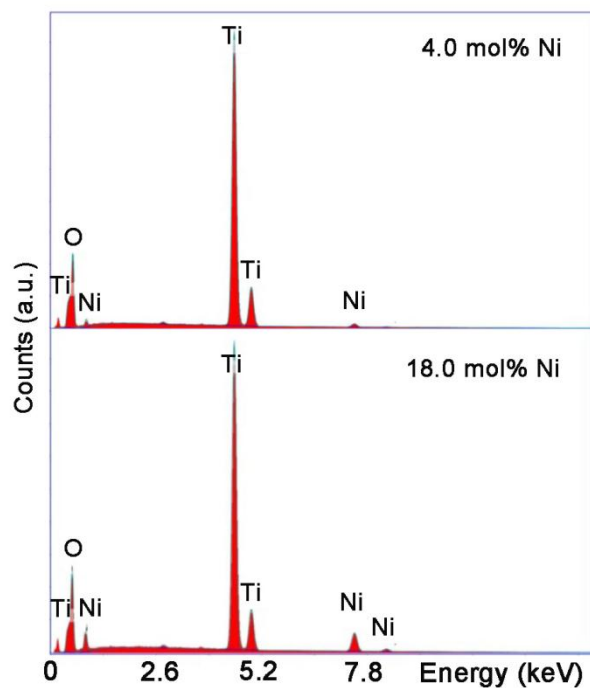


Fig. 3. The EDS spectra of the Ni²⁺-doped TiO₂ samples with different doping concentrations.

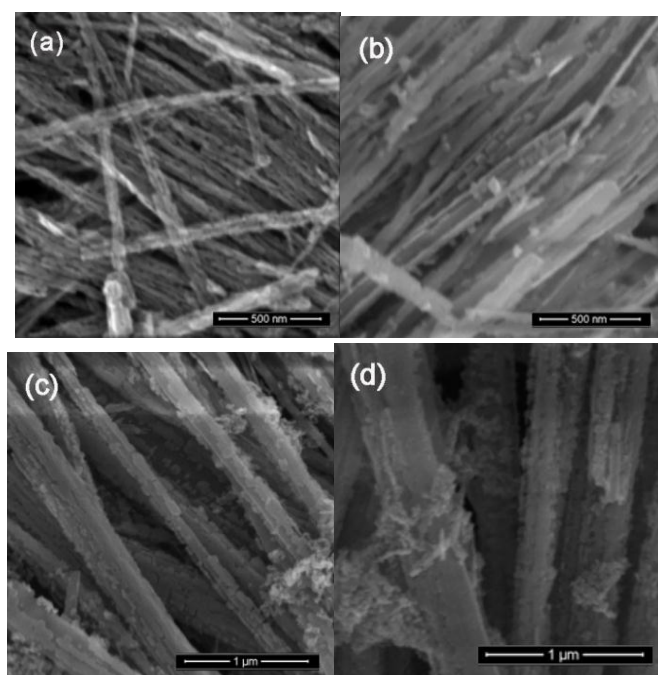


Fig. 4. The FESEM images of the Ni²⁺-doped TiO₂ samples with different doping concentrations: a) 0.5 mol% Ni²⁺, b) 4.0 mol% Ni²⁺, c) 12 mol% Ni²⁺ and d) 18 mol% Ni²⁺.

3.2. Morphology

Fig. 4 shows the FESEM images of the Ni^{2+} -doped TiO_2 nanowires with different doping concentrations. From the images, it is clear that the nanowire diameter significantly increases with increasing the Ni dopant concentration. Namely, average nanowire diameters were found to be 45 ± 5 , 70 ± 5 , 200 ± 25 , and 250 ± 25 nm for the samples doped with 0.5, 4.0, 12.0, and 18.0 mol% Ni^{2+} , respectively.

3.3. Absorption

The diffuse reflectance spectra of $\text{TiO}_2:\text{Ni}^{2+}$ with different doping concentrations are shown in Fig. 5a. As shown in this figure, the reflectivity in the range from 2.0 to 3.8 eV decreases (hence absorption is increased) with increasing Ni^{2+} dopant content. Fig. 5b shows the Kubelka-Munk functions $F(R)$ of the $\text{TiO}_2:\text{Ni}^{2+}$ samples obtained from the diffuse reflection data.

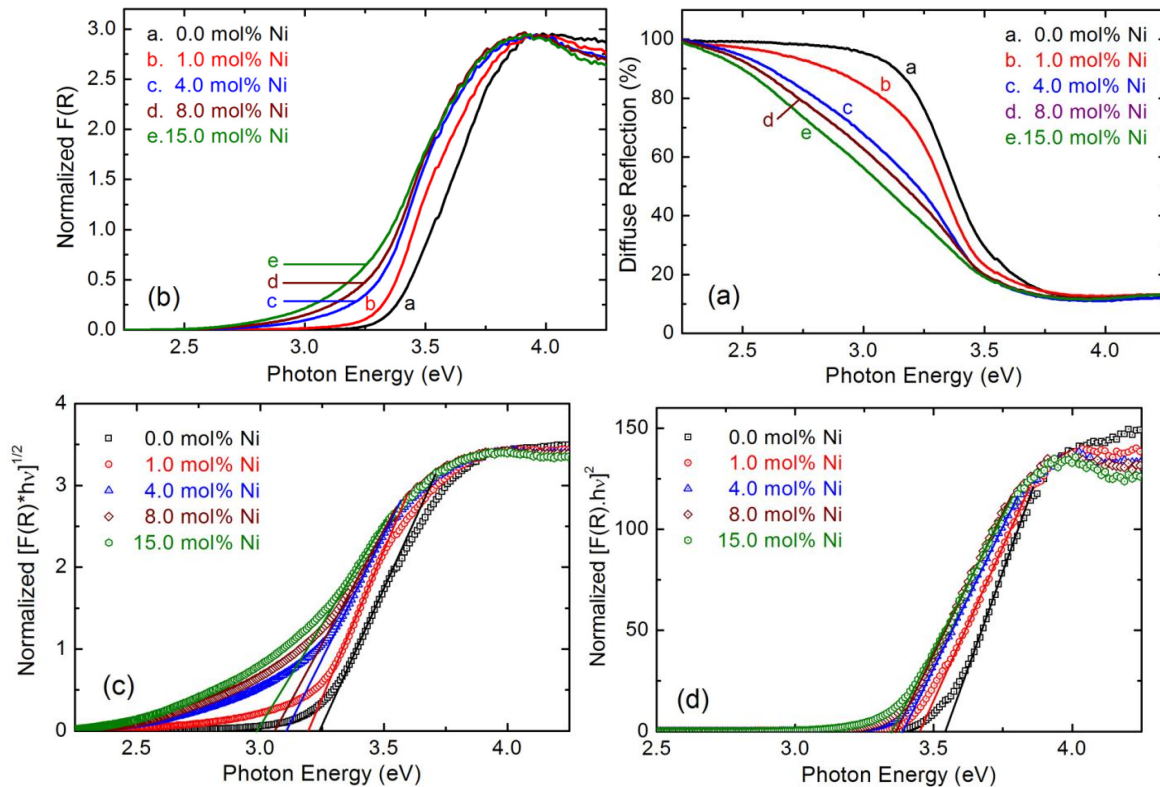


Fig. 5. (a) Diffuse reflectance spectra of $\text{TiO}_2:\text{Ni}^{2+}$ with different concentrations, (b) Kubelka-Munk functions deduced from diffuse reflectance spectra, (c) plots of $[F(R)hv]^{1/2}$ and (d) plots of $[F(R)hv]^2$ versus photon energy $h\nu$.

It is well known that the band gap energy (E_g) is considered one of the important parameters of optical materials [12]. The top of the valence band of the anatase single crystals has two maxima at M and Γ points, which are separated by a very small energy difference, only approximately 2 meV, and the bottom of the conduction band at Γ point [13]. The $\Gamma(\text{VB}) \rightarrow \Gamma(\text{CB})$ transitions are direct, but the $\text{M}(\text{VB}) \rightarrow \Gamma(\text{CB})$ transitions are indirect [13]. For determining band gap energies of the synthesized samples, $[F(R)hv]^{1/2}$ and $[F(R)hv]^2$ are plotted against $h\nu$ for the indirect and direct transitions,

respectively. The lines drawn on the linear part of $[F(R)hv]^{1/2}$ and $[F(R)hv]^2$ versus hv at $[F(R)hv]^{1/2} = 0$ and $[F(R)hv]^2 = 0$ give the indirect and direct band gap energy, respectively. For the undoped TiO_2 samples, we have obtained the values 3.24 and 3.54 eV corresponding to the indirect and direct band gap, respectively. These results are larger than experimental values for the band gap energy of anatase TiO_2 nanopowders reported by Trenczek-Zajac et al. [14], but are in good agreement with the calculated values obtained by Zielinska et al. [15], and the experimental values (3.20 and 3.53 eV) for TiO_2 nanoparticles reported by Reyes-Coronado et al. [16]. The band gap energy values obtained for the indirect and direct transitions of our TiO_2 nanowires with different Ni^{2+} dopant contents are summarized in Table 2. The results indicate that the band gap of the TiO_2 nanowires is decreased with increasing Ni^{2+} dopant content. It is generally accepted that most of the transition metal energy levels exist between the valence and conduction bands of TiO_2 [8, 11, 12, 17]. Therefore, a possible electronic transition from Ni^{2+} energy level to the conduction band of TiO_2 is considered a main reason for reducing the band gap energy. Beside, the transition metals could also make significant changes on the electronic structure of a crystalline material and thus on the values of the gap energy [18].

Table 2. Variations of the band gap energy with Ni-doped TiO_2 samples

Ni^{2+} dopant content (mol%)	E_g (eV)	
	Indirect transitions	Direct transitions
0	3.24	3.54
1	3.20	3.45
4	3.11	3.39
8	3.06	3.36
15	2.99	3.35

4. Conclusion

Nanowires of $TiO_2:Ni^{2+}$ were successfully obtained by hydrothermal technique from precursors of anatase TiO_2 , urea powders, $Ni(NO_3)_2$ and NaOH aqueous solutions. XRD and Raman analysis indicated that all the synthesized nanowires exhibit anatase single phase. The lattice parameters and mode Raman positions are independents on Ni^{2+} dopant contents. While, the FESEM images show that the diameter of TiO_2 nanowires increased significantly with increasing concentrations of Ni^{2+} . The diffuse reflection spectra were used to determine both the indirect and direct band gap energy of TiO_2 nanowires as a function of the concentration of Ni^{2+} ions. The results indicated that band gap decreases with increasing Ni^{2+} content.

Acknowledgments

This work is financially supported by Vietnam National University (Project No. QG.14.15).

References

- [1] A. Fujishima, X. Zhang, D. A. Tryck, Surface Science Reports 63 (2008) 515–582
- [2] M.I. Baraton, Recent Pat. Nanotechnol. 6 (2012) 10.
- [3] V. Galstyan, E. Comini, G. Faglia and G. Sberveglieri, Sensors 13(2013) 14813-14838.
- [4] X. Chen and S. S. Mao, Chem. Rev., 107 (7) (2007) pp 2891–2959.

- [5] C. Dette, M.A. Perez-Osorio, C. S. Kley, P. Punke, C. E. Patrick, P.Jacobson, F. Giustino, S. J. Jung, and K. Kern, *Nano Lett.*, 14 (11) (2014) 6533–6538
- [6] X. Chen, L.Liu, P.Y. Yu, S.S. Mao. *Science* 331 (2011) 746-750.
- [7] S. Valencia, J.M. Marin and G. Restrepo, *The Open Materials Science Journal* 4 (2010) 9-14
- [8] Trinh Thi Loan, Nguyen Ngoc Long, *VNU Journal of Science: Mathematics – Physics*, Vol. 30, No. 2 (2014) 59-67.
- [9] D. Jing, Y. Zhang, L. Guo, *Chemical Physics Letters* 415 (2005) 74–78.
- [10] T. Ohsaka, E. Izumi, Y. Fujiki, *J. Raman Spectrosc.* 7 (1978) 321-324.
- [11] A. K. Tripathi, M. C. Mathpal, P. Kumar, V. Agrahari, M. K. Singh, S. K. Mishra, M. M. Ahmad, A. Agarwal, *Adv. Mater. Lett.* 6(3) (2015) 201-208.
- [12] M.A. Ahmed, E.E. El-Katori, Z. H. Gharni, *Journal of Alloys and Compounds* 553 (2013) 19–29.
- [13] S.D. Mo and W. Y. Ching, *Phys. Rev.* 51(1995) 13023-13032.
- [14] A. Trenczek-Zajac, M. Radecka, M. Jasinski, K.A. Michalow, M. Rekas, E. Kusior, K. Zakrzewska, A. Heel, T. Graule, K. Kowalski, *Journal of Power Sources* 194 (2009) 104–111.
- [15] M. Landmann, E. Rauls and W. G. Schmidt, *J. Phys.: Condens. Matter* 24 (2012) 195503 (6pp).
- [16] D Reyes-Coronado, G Rodríguez-Gattorno, M E Espinosa-Pesqueira, C Cab, R de Coss and G Oskam, *Nanotechnology* 19 (2008) 145605.
- [17] B. Choudhury, M. Dey and A. Choudhury, *International Nano Letters* 3 No.1 (2013) 1-8.
- [18] A. Hajjaji, A. Atyaoui, K. Trabelsi, M. Amlouk, L. Bousselmi, B. Bessais, M.A.E. Khakani and M. Gaidi, *American Journal of Analytical Chemistry* 5 (2014) 473-482.